

Electron beam irradiation on novel coronavirus (COVID-19): A Monte–Carlo simulation*

Guobao Feng(封国宝)¹, Lu Liu(刘璐)², Wanzhao Cui(崔万照)^{1,†}, and Fang Wang(王芳)³

¹National Key Laboratory of Science and Technology on Space Microwave, China Academy of Space Technology, Xi'an 710000, China

²School of Computer Science and Engineering, Xi'an University of Technology, Xi'an 710048, China

³Key Laboratory for Physical Electronics and Devices of the Ministry of Education, Xi'an Jiaotong University, Xi'an 710049, China

(Received 17 February 2020; revised manuscript received 20 February 2020; accepted manuscript online 9 March 2020)

The novel coronavirus pneumonia triggered by COVID-19 is now raging the whole world. As a rapid and reliable killing COVID-19 method in industry, electron beam irradiation can interact with virus molecules and destroy their activity. With the unexpected appearance and quickly spreading of the virus, it is urgently necessary to figure out the mechanism of electron beam irradiation on COVID-19. In this study, we establish a virus structure and molecule model based on the detected gene sequence of Wuhan patient, and calculate irradiated electron interaction with virus atoms via a Monte Carlo simulation that track each elastic and inelastic collision of all electrons. The characteristics of irradiation damage on COVID-19, atoms' ionizations and electron energy losses are calculated and analyzed with regions. We simulate the different situations of incident electron energy for evaluating the influence of incident energy on virus damage. It is found that under the major protecting of an envelope protein layer, the inner RNA suffers the minimal damage. The damage for a ~ 100 -nm-diameter virus molecule is not always enhanced by irradiation energy monotonicity, for COVID-19, the irradiation electron energy of the strongest energy loss damage is 2 keV.

Keywords: electron beam irradiation, novel coronavirus (COVID-19), numerical simulation

PACS: 87.15.-v, 61.80.Fe, 52.65.Pp

DOI: 10.1088/1674-1056/ab7dac

1. Introduction

A novel coronavirus spread from a seafood market in Wuhan is now raging the whole world, especially in China.^[1] So far, more than 3000 people have been killed, and more than 100000 people are infected, billions of people have to isolate at home to avoid cross infection.^[2] Kinds of disinfectant are used to kill virus, such as medicinal alcohol, iodine and even suds.^[3] In industry, ray and particle radiation can be used to kill bacteria and virus quickly and effectively.^[4–6]

Electron beam irradiation with a special advantage can inactivate moribund microorganisms which attach the foods, while has less impact on product quality. As reported by Luchsinger *et al.*,^[7] electron beam irradiation can kill *Escherichia coli* and *salmonella* in pork, and was thought to have huge potential on protecting food safety.

For COVID-19, since recent researches indicate that the main transmission methods are spray and attachment, viruses will finally stay at the surface of object. Comparing with the method of microwave heating for killing virus, the electron beam irradiation with several keV energy just can focus energy loss on surface viruses more effectively. In addition, the electron beam irradiation can also be applied in the virus related vaccine development for accurate inactivation, electron microscopy imaging analysis of virus structure.^[8–10] Al-

though many investigations about electron irradiation on virus have been carried out around the world,^[11–14] owing to the rapid outbreak of the novel coronavirus disaster, realization of the novel coronavirus (COVID-19) is still not enough. How does the irradiated electron interact with the novel coronavirus (COVID-19) is still unclear. Consider the experiment of electrons irradiating the novel coronavirus is hardly to achieve in the present stage, theoretical investigation via numerical simulations comes to be a feasibility important method.^[15,16]

Hence, in this study, we investigate the characteristics of interaction of an irradiated electron beam with the novel coronavirus (COVID-19) via a Monte Carlo numerical simulation. The physical model of COVID-19 is built based on the detected gene sequence of Wuhan patient from the National Center for Biotechnology Information (NCBI). The interactions including elastic and inelastic scattering between irradiated electrons and RNA/protein molecule are calculated with Mott and Rutherford mode. Characteristics of internal electrons and excitation distribution are simulated. For better understanding the impact of E-beam irradiation on each part of COVID-19, we still analyzed excitations and energy loss in each area. Furthermore, variation of energy loss in each area in different situations of incident energy is investigated for indicating the sensitivity of energy on COVID-19.

*Project supported by the National Natural Science Foundation of China (Grant No. 61901360).

†Corresponding author. E-mail: cuiwanzhao@126.com

2. Models and methods

2.1. Virus structure model

Since the novel coronavirus (COVID-19) has many kinds of surrounding function proteins,^[17] for the feasibility of calculation, here we choose three kinds of mainly proteins when building the physical model with a reasonably simplify. Similar to other discovered coronavirus such as SARS and MERS, the novel coronavirus (COVID-19) is firstly surrounded by some sparse spike glycoproteins as shown in Fig. 1. Then, under the spike glycoproteins, there is more than one layer of envelope proteins. Although there is still a fraction of hemagglutinin in this area to help fuse viruses to cells,^[18] in our physical model we pick the main envelop proteins as a represen-

tative. Inside the novel coronavirus, the nucleocapsid closely attach the RNA, both of them are wandering inside the virus together with a gap space. Considering the complexity of RNA space structure and randomness of RNA movement, hence in our physical model, we can treat them as nucleocapsid surround RNA in a uniform region. Constituent parts including spike glycoproteins, envelope, nucleocapsid and RNA are represented as M1, M2, M3, and M4, respectively. As reported by the Centers for Disease Control and Prevention (CDC), the COVID-19 is a large sized virus whose diameter is approximately 120 nm.^[19] Hence, in this study, the external/inner diameter of M1–M3 are set to be 120/100 nm, 100/80 nm, 60/50 nm, and the RNA(M4) is in the range of 50 nm diameter space.

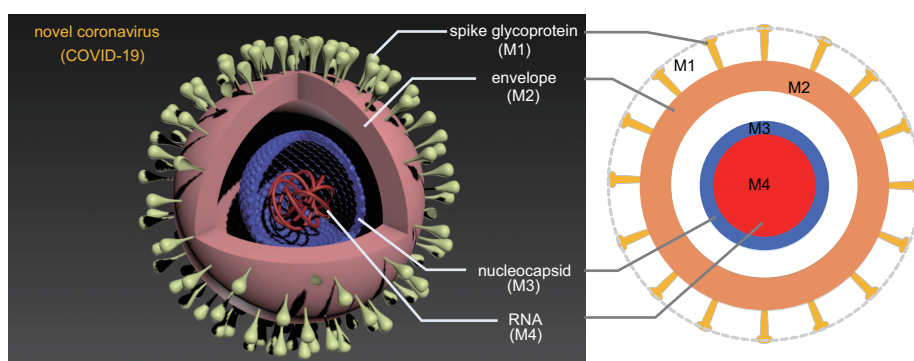


Fig. 1. The novel coronavirus (COVID-19) 3D structure and its simplified physical structure model.

Table 1. Statistical data of 20 amino acid sequences of three kinds of proteins from NCBI.

Amino acid	Molecular formula	Spike protein				Envelope protein				Nucleocapsid protein			
		Number	Proportion	Average molecular weight	Average molecular formula	Number	Proportion	Average molecular weight	Average molecular formula	Number	Proportion	Average molecular weight	Average molecular formula
Glycine, G	C ₂ H ₅ O ₂ N ₁	82	6.94%			14	6.81%			43	10.64%		
Alanine, A	C ₃ H ₇ O ₂ N	79	6.71%			19	9.06%			37	9.23%		
Leucine, L	C ₆ H ₁₃ O ₂ N	108	8.98%			35	16.27%			25	6.40%		
Isoleucine, I	C ₆ H ₁₃ O ₂ N	76	6.47%			20	9.51%			14	3.80%		
Valine, V	C ₅ H ₁₁ O ₂ N	97	8.12%			12	5.91%			8	2.39%		
Proline, P	C ₅ H ₉ O ₂ N	58	5.06%			5	2.75%			28	7.10%		
Phenylalanine, F	C ₉ H ₁₁ O ₂ N	77	6.55%			11	5.45%			13	3.57%		
Methionine, M	C ₅ H ₁₁ O ₂ NS	14	1.60%			4	2.30%			7	2.15%		
Tryptophan, W	C ₁₁ H ₁₂ O ₂ N ₂	12	1.44%			7	3.65%			5	1.68%		
Serine, S	C ₃ H ₇ O ₃ N	99	8.28%	128.89	C(4.9458)	15	7.26%	131.19	C(5.2297)	37	9.23%	124.42	C(4.6108)
Glutamine, Q	C ₅ H ₁₀ O ₃ N ₂	62	5.37%		H(9.6732)	4	2.30%		H(10.203)	35	8.75%		H(9.2925)
Threonine, T	C ₄ H ₉ O ₃ N	97	8.12%		O(2.4870)	13	6.36%		O(2.3514)	32	8.05%		O(2.4505)
Cysteine, C	C ₂ H ₇ O ₂ NS	40	3.64%		N(1.1987)	4	2.30%		N(1.2523)	0	0%		N(1.3042)
Asparagine, N	C ₄ H ₈ O ₃ N	88	7.41%		S(0.04242)	11	5.45%		S(0.03604)	22	5.69%		S(0.01651)
Tyrosine, Y	C ₉ H ₁₁ O ₃ N	54	4.74%			9	4.55%			11	3.09%		
Aspartic acid, D	C ₄ H ₇ O ₄ N	62	5.37%			6	3.20%			23	5.92%		
Glutamic acid, E	C ₅ H ₉ O ₄ N	48	4.27%			7	3.65%			12	3.33%		
Lysine, K	C ₆ H ₁₄ O ₂ N ₂	61	5.29%			7	3.65%			31	7.81%		
Arginine, R	C ₆ H ₁₄ O ₂ N ₃	42	3.80%			14	6.81%			29	7.34%		
Histidine, H	C ₆ H ₉ O ₂ N ₃	17	1.84%			5	2.75%			4	1.44%		

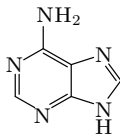
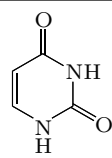
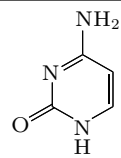
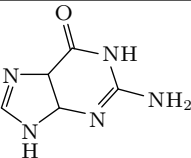
For molecular formulas of each constituent parts in the novel coronavirus, we pick and count typical gene sequences of three kinds of proteins and RNA of Wuhan patient from the National Center for Biotechnology In-

formation (NCBI). The sequences of spike glycoproteins (M1) of COVID-19 are picked from Wuhan-Hu-1 (reference sequence: NC_045512.2),^[20] the sequences of envelope (M2), nucleocapsid (M3) and RNA (M4) are picked

from Wuhan-Hu-1 (GenBank: MN908947.3).^[21] Table 1 denotes statistical results of 20 amino acid sequences of three kinds of proteins. The average molecular weight of three kinds of proteins (spike proteins (M1), envelope (M2), nucleocapsid (M3)) are 128.89, 131.19, and

124.42, respectively. The average molecular formula of three kinds of proteins (spike proteins (M1), envelope (M2), nucleocapsid (M3)) are $C_{4.9458}H_{9.6732}O_{2.4870}N_{1.1987}S_{0.0424}$, $C_{5.2297}H_{10.203}O_{1.2523}N_{2.3514}S_{0.0360}$ and $C_{4.6108}H_{9.2925}O_{2.4505}N_{1.3042}S_{0.0165}$, respectively.

Table 2. Statistical data of 4 nucleobase sequences of an original RNA from NCBI.

RNA Nucleobase	Adenine	Uracil	Cytosine	Guanine
Molecular structure				
Molecular formula	$C_5H_5N_5$	$C_4H_4O_2N_2$	$C_4H_5ON_3$	$C_5H_5ON_5$
Number	8954	9594	5492	5863
Proportion	29.94%	32.08%	18.37%	19.61%
Average molecular weight	126.46			
Average molecular formula	$C_{4.50}H_{4.68}O_{1.02}N_{3.67}$			

2.2. Physical calculation model

When an incident electron irradiates inside COVID-19, a series of collision process between energetic electrons and the virus structure molecule will occur. Based on the energy loss situation, the collision process can be divided into elastic scattering process without energy loss and inelastic scattering process with energy loss.^[22] In this study, we calculate the elastic scattering process with Rutherford mode, and handle the inelastic scattering process with the fast secondary electron (FSE) mode. We should track each electron (including incident electron and generated secondary electron) until its energy depleted or outgoing from the virus surface with a Monte Carlo numerical simulation.

For elastic scattering process, it is necessary for us to obtain scattering angle during the collision between electron and atoms. Here we use the Rutherford mode to calculate the elastic scattering cross section σ_e

$$\sigma_e = 5.21 \times 10^{-21} \frac{z^2}{E^2} \frac{4\pi}{\alpha(1+\alpha)} \left(\frac{E+511}{E+1022} \right)^2,$$

where E is electron energy, z is the number of atoms, α is the shielding factor that denotes the shielding ability of outer electron on nucleus. For the COVID-19 molecule who is a polyatomic molecule, the atom number can be treated as the average atom number.

For the inelastic scattering process, we should consider not only the change of angle but also the transfer of energy.^[23] Based on the FSE mode, the inelastic scattering cross section σ_{in} when considered quantum spinning mechanism can be expressed as follows:

$$\sigma_{in} = \int_{\Omega_c}^{0.5} \left(\frac{d\sigma}{d\Omega} \right)_M = \frac{\pi e^4}{E^2} \left\{ \frac{1}{\Omega_c} - \frac{1}{1-\Omega_c} + \ln \left(\frac{\Omega_c}{1-\Omega_c} \right) \right\}.$$

Here e is the elementary charge, Ω_c is the lower limit of normalized energy loss coefficient. Based on the inelastic scattering cross section we can obtain mean free path and scattering angle during the inelastic collision.

Apart from variation of direction, the energy of electron will transform during the inelastic scattering.^[24,25] Here we can use the continuous slowing down approximation (CSDA) method to calculate the energy loss in each step. The energy loss dE/dS can be calculated by Bethe mode,

$$\left(\frac{dE}{dS} \right)_{\text{Bethe}} = 78500 \frac{\rho Z}{AE} \ln \left(\frac{1.166(E+kJ)}{J} \right),$$

where ρ is the material density, z is the atom number, and A is the atomic weight, k is the correction factor, J is the ionization energy. For COVID-19, z , A and J should be the average atom number, average atomic weight and mean ionization energy.

When electron incident virus, a series of Monte Carlo methods will judge what kind of scattering will occur in each collision based on random numbers and scattering feature.

3. Results and analyses

During inelastic scattering between energetic electrons and COVID-19 atoms, part of electron energy may transform to the atoms and results in atom ionization and inner secondary electron generation. A mass of atom ionizations will break the molecular chain and destroy COVID-19 activity.

3.1. Ionization distribution

Figure 2 shows the ionization situations in the COVID-19 sphere under two kinds of incident conditions, point irradiation and uniform irradiation. For better demonstrating the ionization feature, the default irradiated electron number is set to be 20000. The default incident electron primary energy is

set to be 10 keV. Since the incident electrons and generated inner secondary electrons will occur in a series of inelastic ionization processes, the final ionization amount is much larger than the incident electron numbers. From the point irradiation shown in Fig. 2(a), we can find that after suffering a string of collision processes, the intensity of ionization comes to be more divergency, while this tendency is equalized in the situation of uniform irradiation Fig. 2(b). In the broadside, the ionization intensity appears to be fewer because the electrons are easier to escape and thus lots of cascade collisions release.

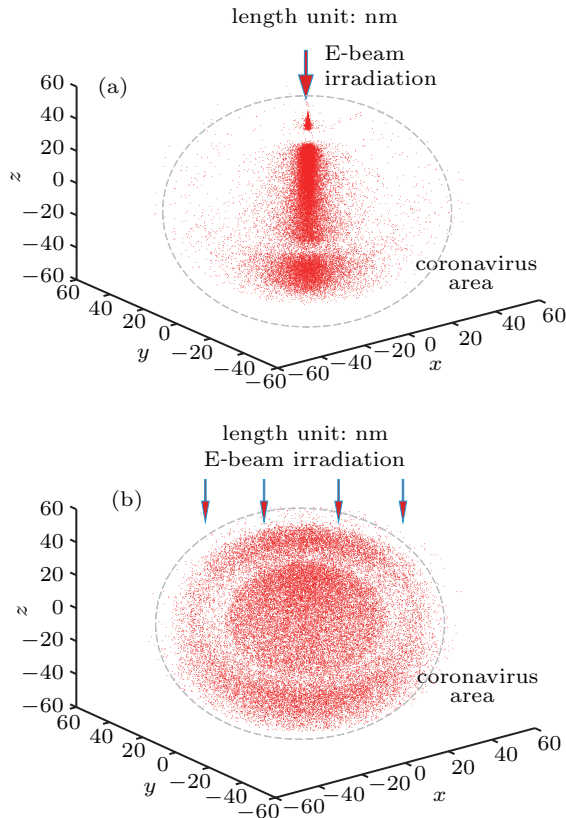


Fig. 2. Atom-ionization 3D distribution in the COVID-19 sphere under point and uniform E-beam irradiation: (a) point irradiation, (b) uniform irradiation.

Each of inelastic scattering caused ionization will excite a pair of free electron and hole. Figure 3 denotes the excitation distribution in both irradiation direction z and virus sphere radial direction R . The E-beam incident condition is in default uniform irradiation. For Fig. 3(a), the irradiation point is at $z = 60$ nm, and the tendency of decrease in both ends can be explained by variation of valid cross-sectional volume.

As shown in radial direction in Fig. 3(b), we can intuitively obtain the ionization situation in every four areas. Since spike proteins sparsely distribute around the outermost shell, the ionization it suffered is not high as denoted in the M1 area. The major excitation occurs in M2 as denoted, which means the envelope layer suffers the most irradiation ionization. Af-

ter skipping over a gap space, the nucleocapsid (M3) still suffers a high E-beam irradiation ionization, while the ionization of RNA (M4) rapid recedes with R in the central of virus COVID-19.

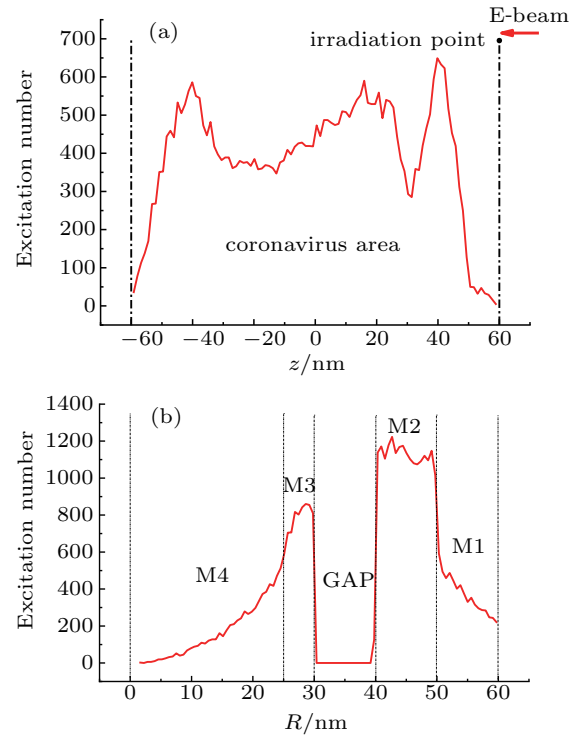


Fig. 3. excitation number distribution in irradiation direction z (a) and radial direction R (b).

3.2. Energy loss

When the energetic electron exhibits inelastic scattering with an atom, a part of electron energy loss results in excitation of free-electron pairs, while another part of electron energy loss may transform to phonon which may lead to geometry structural damage. Hence, for accurately evaluating the influence of E-beam irradiation on virus, we should also investigate the characteristics of electron energy loss.

Figure 4(a) is the normalized electron energy loss spectrum in the whole COVID-19. Although the incident primary electron energy is as high as 10 keV, the mainly electron energy loss focused on 10 eV to 87 eV reaches as much as 78.4%. Hence, if a 10 keV incident electron depletes its energy within one virus, it needs about hundreds of inelastic scattering, which is scarcely possible for a ~ 100 -nm-diameter COVID-19. Since each electron energy loss does always comes from excitation of free electron and hole, the times of electron energy loss are much larger than the excitation number, as shown in Fig. 4(b). The overall tendency of distribution of energy loss times in radial direction is similar to the excitation number distribution, owing to high randomness and denseness, the curve of energy loss distribution is more smoothness.

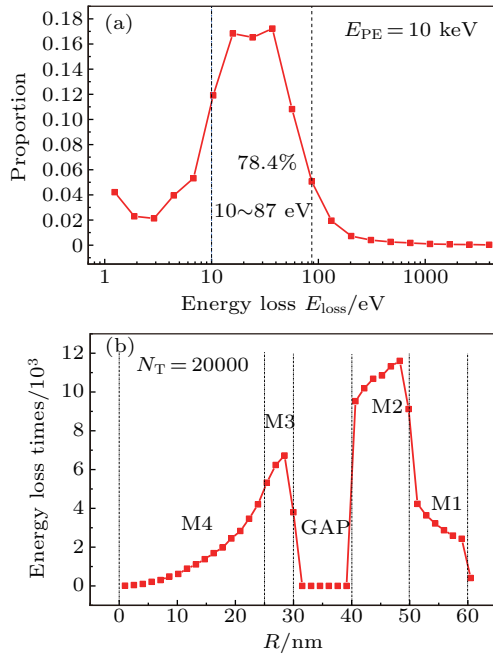


Fig. 4. Normalized energy loss spectrum (a) and energy loss distribution in radial direction R (b).

Because of differences in molecular formula and space structure in the four areas, the energy loss spectrum and the total energy loss will appear to be different. Figure 5(a) is the normalized electron energy loss spectrum in M1, M2, M3 and M4 presented with black, red, blue and green dotted lines. From the energy loss spectrum curve of M2 in Fig. 5(a), we can find that its peak energy loss is larger than other three areas, which results in the double-peak curve in Fig. 4(a). A larger peak energy loss of M2 means that electron may lose more energy when across a unit length in envelope compared with others. After integrating all of loss energies in each area, the total energy loss in M1–M4 is shown in Fig. 5(b). Values of total energy loss TE_{loss} in M1–M4 are 7.6×10^5 eV, 2.8×10^6 eV, 8.4×10^5 eV and 7.0×10^5 eV. The envelope protein M2 suffers the most electron energy loss damage, while

protects the RNA M4 suffer the least electron energy loss damage.

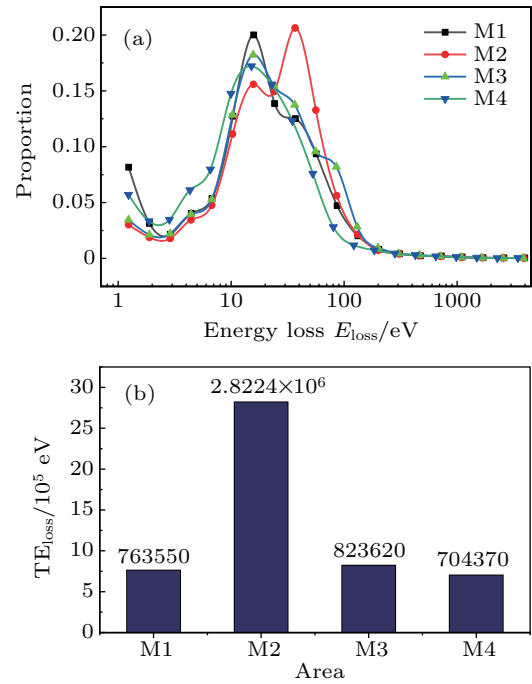


Fig. 5. Normalized energy loss spectrum (a) and the total energy loss TE_{loss} (b) in the four areas.

3.3. Primary energy

Considering electrons with different energies may occur diverse collision processes, E-beam irradiation with different primary energy also has different impact on virus COVID-19. Figure 6 shows the atom ionization 3D distribution and the excitation number distribution under four different incident conditions: 1 keV, 5 keV, 10 keV, and 20 keV. Incident electron numbers of the four conditions are also set to be default 20000. We can find that when the incident energy is as low as 1 keV, the incident electrons can not reach all virus area, only the upper area

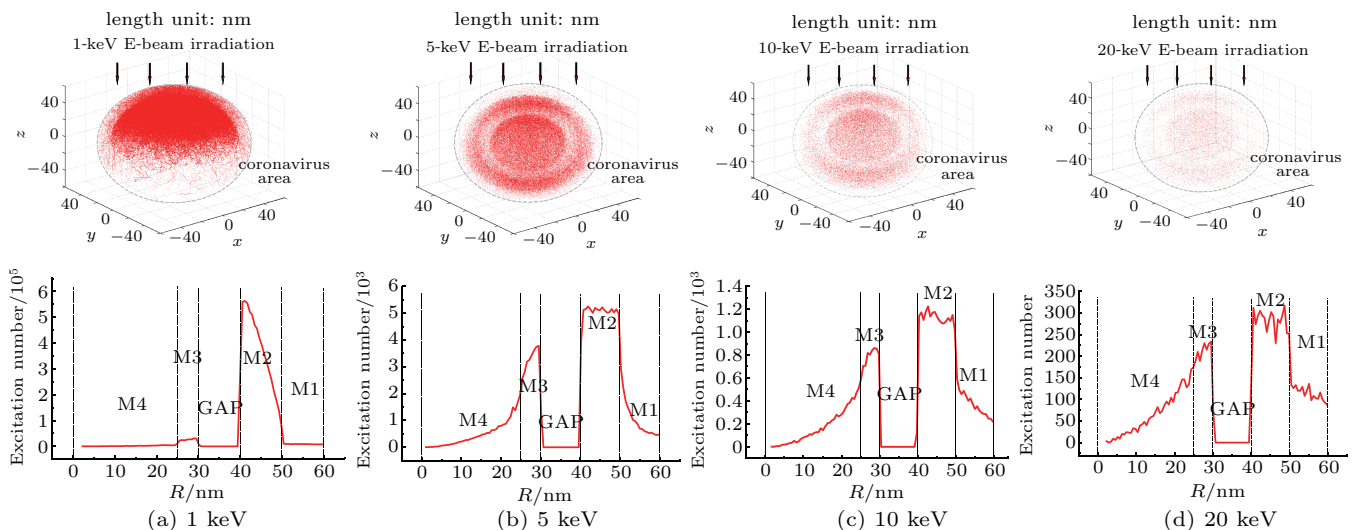


Fig. 6. Atom ionization 3D distribution and excitation number distribution in radial direction under different incident primary energies: (a) 1 keV, (b) 5 keV, (c) 10 keV, (d) 20 keV.

appears to be of ionization. Most of the electron-hole excitation occurs in M2, and the electron irradiation damage can be resisted by envelope protein. When the incident energy rises to 5 keV, incident electrons can reach all of the virus area. As the incident energy keeps enhancing, the ionization number decreases and distribution shifts toward inner.

After integrating the energy loss in each area under different incident energies, in the major resistance area M2, the energy loss decreases with incident energy because a larger energy electron can more easily across the envelope layer, which also results in the total energy loss decreasing with incident energy when the incident energy is larger than 2 keV. As a core of virus, because under protects of multilayer, the energy loss of RNA M4 appears to be very weak when the incident energy is 1 keV. With the increase of incident energy, the energy loss in RNA M4 first enhances and then decreases. This is mainly because, on the one hand, a larger energy electron has more possibility to reach the RNA M4 area, on the other hand, a larger energy also has a longer mean free path that corresponds to less collision times. For COVID-19, when the incident electron energy is 2 keV, the damage resulted by collision energy loss reaches the maximum. We define the damage efficiency to be the ratio of the total loss energy in virus to the total incident energy, as shown in Fig. 7(b) with blue percentage. The damage efficiency when incident energy is 2 keV can still reach 55%.

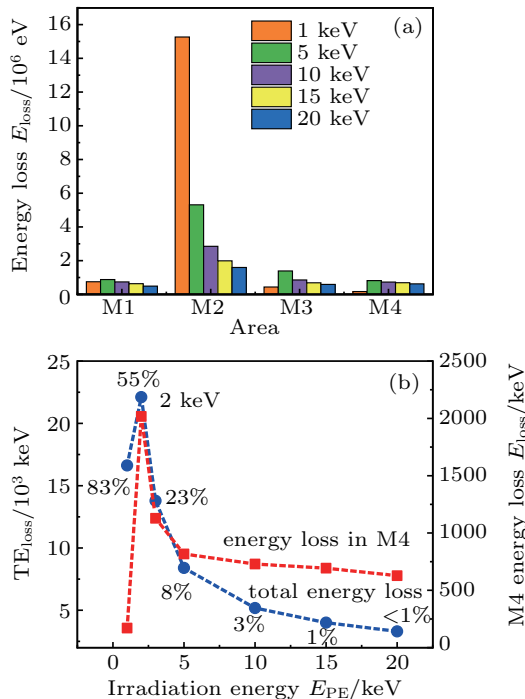


Fig. 7. Energy loss in areas (a) and variation of total energy loss with irradiation energy (b).

3.4. Surrounding environment

Considering the exhausted COVID-19 always appears in the form of surrounding aerosol environment, we should ana-

lyze the resistance effects of surrounding environment on electron beam irradiation penetration. The surrounding aerosol is a suspension of fine airborne solid or liquid particles in gas whose typical layer thickness is less than several micrometers. Here we pick the liquid H₂O as the main component of surrounding environment.

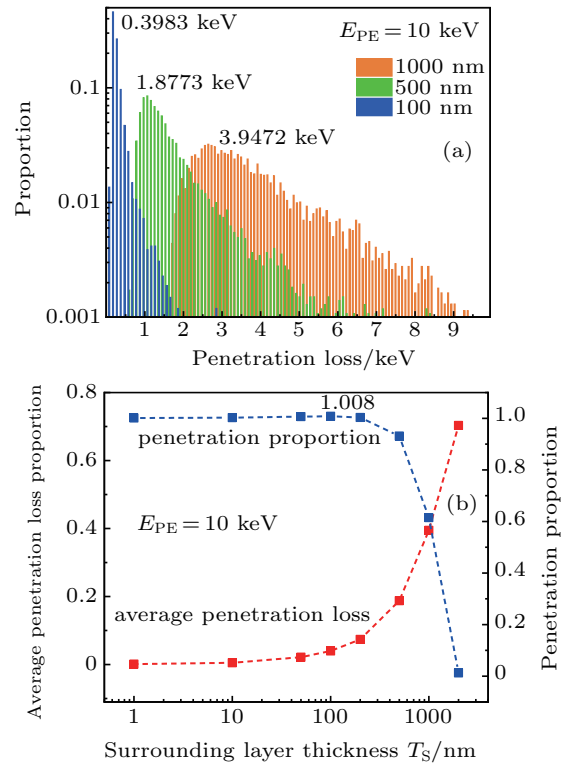


Fig. 8. Electron penetration loss in COVID-19 surrounding environment: (a) penetration loss spectrum, (b) different surrounding layer thickness situations.

Figure 8(a) shows the irradiated electron energy loss when across the surrounding H₂O layer in three different thickness situations: 100 nm, 500 nm and 1000 nm. Because of a longer layer thickness comes from a more collision process, the primary electron energy can be continuous dissipation, and the penetration loss spectrum appears to be flatter, such as 1000 nm situation. For the situation of a thinner surrounding layer, there are still a small amount of low energy penetration electrons, which are mainly excited secondary electrons near the edge. When the primary electron energy is 10 keV, the average penetration losses for the 100 nm, 500 nm and 1000 nm thick layers are 0.3983 keV, 1.8773 keV, and 3.9472 keV, respectively. Average penetration loss proportion defined as ratio of loss energy in primary energy linearly increases with layer thickness. Although a thicker layer results in a larger energy loss, the penetration electron number does not monotonously decreases with layer thickness for the generation of excited secondary electrons. As shown in Fig. 8(b), the penetration proportion reaches 1.008 in the case of layer thickness 100 nm, which means that the penetration electron number is larger than the incident electron number. When the

layer thickness is larger than 1000 nm, the penetration proportion rapidly decreases. In industry, if the virus is pre-placed in a dry environment for evaporating the surrounding layer, the protection of surrounding layer on virus will be effectively suppressed.

4. Conclusions

We have investigated the interaction between irradiated electrons and the novel coronavirus COVID-19 with a Monte Carlo numerical simulation. After modeling the COVID-19 molecular structure and scattering processes, we obtain the following conclusions. Under the electron irradiation, the major ionization damages occur in the envelope protein layer for protecting the inner RNA. The energy loss of electrons interacting with COVID-19 atoms focuses on 10–87 eV reaching 87%. The peak energy loss of envelope protein appears to be larger than other parts of virus. Although a higher energy electron can help to deepen, the total energy loss damage of COVID-19 first enhances and then recedes for a longer mean free path in higher energy situation. The irradiation electron energy corresponding to the strongest energy loss damage is around 2 keV, whose damage efficiency can reach 55%. This study can provide a theoretical support on COVID-19 inactivation with a rapid and reliable approach in researches and industries. We hope this plague will terminate soon.

References

- [1] Guan W J, Ni Z Y, Hu Yu *et al.* 2020 *New Engl. J. Med.* (in press)
- [2] <http://www.nhc.gov.cn/wjw/zxfb/list.shtml>
- [3] Van E, Terpstra F G and Schuitemaker H 2002 *J. Hosp. Infect.* **51** 121
- [4] Nevelsky A, Borzov E and Daniel S 2017 *J. Appl. Clin. Med. Phys.* **18** 196
- [5] Jasmin F, Lea B, Thomas G *et al.* 2013 *Viruses* **8** 319
- [6] Smolko E E and Lombardo J H 2005 *Nucl. Instrum. Meth. B* **236** 249
- [7] Luchsinger S E, Kropf D H, García-Zepeda C M *et al.* 2006 *J. Food Sci.* **61** 1000
- [8] Lea B, Jasmin F and Sebastian U 2018 *Vaccine* **36** 1561
- [9] Sabbaghi A, Miri S M, Keshavarz M *et al.* 2019 *Rev. Med. Virol.* **29** 2074
- [10] <https://www.niaid.nih.gov/news-events/novel-coronavirus-sarscov2-images>
- [11] Brahmakshatriya V, Lupiani B and Brinlee J L 2009 *Avian. Pathol.* **38** 245
- [12] Chandni P, Brooke A D and David H K 2013 *Appl. Environ. Microb.* **79** 3796
- [13] Tanja S, Arnd T H and Uwe G 2012 *Transfus. Med. Hemoth.* **39** 29
- [14] Zhang T, Li Z and Tao J 2013 *Chin. Animal Health Inspection* **30** 52 (in Chinese)
- [15] Xu X T, Chen P and Wang J F, Feng J N, Zhou H, Li X, Zhong W and Hao P 2020 *Sci. Chin. Life Sci.* **63** 457
- [16] Xu Z J, Peng C and Shi Y L 2020 *Sci. Chin. Life Sci.* (in press)
- [17] Lu R J, Zhao X and Li J 2020 *Lancet* **395** 565
- [18] Malik Y S, Sircar S and Bhat S 2020 *Vet. Quart.* **40** 68
- [19] <https://www.pptaglobal.org/media-and-information/ppta-statements/1055-2019-novel-coronavirus-2019-ncov-and-plasma-protein-therapies>
- [20] https://www.ncbi.nlm.nih.gov/nuccore/NC_045512.2/
- [21] <https://www.ncbi.nlm.nih.gov/nuccore/MN908947>
- [22] Feng G B, Cui W Z and Zhang N 2017 *Chin. Phys. B* **26** 097901
- [23] Feng G B, Liu L and Cui W Z 2019 *IEEE Trans. Plas. Sci.* **47** 3783
- [24] Feng G B, Wang F and Hu T C 2015 *Chin. Phys. B* **24** 117901
- [25] Chang C, Tang C X and Wu J H 2013 *Phys. Rev. Lett.* **110** 064802